Two-Photon Polymerization of Butterfly Wing Scale Inspired Surfaces with Anisotropic Adhesion

Zefu Ren,[∇,†] *Zhuoyuan Yang,*[∇,†] *Rishikesh Srinivasaraghavan Govindarajan,*[†] *Foram Madiyar,*[‡] *Meng Cheng,*[*,§] *Daewon Kim,*[*,†] *and Yizhou Jiang*[*,†]

[†]Department of Aerospace Engineering, Embry-Riddle Aeronautical University, Daytona Beach, FL 32114, United States

[‡]Department of Physical Science, Embry-Riddle Aeronautical University, Daytona Beach, FL 32114, United States

[§] Key Laboratory of Metallurgical Equipment and Control Technology, Ministry of Education, Wuhan University of Science and Technology, Wuhan, Hubei 430081, China

Keywords: butterfly wing scale; bio-inspired microstructures; two-photon polymerization; anisotropic adhesion; additive manufacturing

ABSTRACT

Wings of Morph aega butterflies are natural surfaces that exhibit anisotropic liquid adhesion. The direction-dependent arrangement of wing scales creates orientation-turnable microstructures with two distinct contact modes for liquid droplets. Enabled by recent developments in additive manufacturing, such natural surface designs coupled with hydrophobicity play a crucial role in applications like self-cleaning, anti-icing, and fluidic manipulation. However, the interplay among resolution, architecture, and performance of bio-inspired structures is barely achieved. Herein, inspired by the wing scales of the Morpho aega butterfly, full-scale synthetic surfaces with anisotropic adhesion fabricated by two-photon polymerization are reported. The quality of the artificial butterfly scale is improved by optimizing the laser scanning strategy and objective lens movement path. The corresponding contact angles of water on the fabricated architecture with various design parameters are measured, and the anisotropic fluidic adhesion is investigated. Results demonstrate that tuning the geometrical parameters and spatial arrangement of the artificial wing scales enables anisotropic behaviors of the droplet's motion. The measured results also indicate a reverse phenomenon of the fabricated surfaces in contrast to their natural counterparts, possibly attributed to the significant difference in equilibrium wettability between the fabricated microstructures and the natural Morpho aega surface. These findings are utilized to design next-generation fluid-controllable interfaces for manipulating liquid mobility on synthetic surfaces.

INTRODUCTION

Natural structures found in organisms have evolved over thousands of years to be functionally efficient. Such structures in biosystems can exhibit various properties, including high strength-to-mass ratio, adhesion, fluid direction controllability, and hydrophobicity.[1-5] Particularly, hydrophobic surfaces exist naturally in plants and insects like lotus leaves, rice leaves, beetles, and butterfly wings.[5-8] These structures hold great promise for applications in modern engineering designs and the manufacturing sector. Inspired by natural hydrophobic surfaces, artificial surfaces often exhibit macro to nanoscale hierarchical structures comprising a range of features organized in a structured geometric pattern. The integrated structure composed of ordered features provides the means to manipulate the interfaces and dynamics of liquid-air and liquid-solid interactions. Consequently, the presence of hierarchical microstructures and nanostructures can improve hydrophobicity by promoting high contact angle of water.[9]

With the recent development in additive manufacturing (AM), the fabrication of bio-inspired hydrophobic structures is enabled.[9-11] Many AM techniques, including fused deposition modeling

(FDM), selective laser melting (SLM), and digital light processing (DLP), have been used to rapidly prototype and develop such hydrophobic surfaces. Among them, FDM is an extrusion-based AM method using polymer-based filaments. The filament is melted by passing through a heated nozzle and deposited on a heated platform when the filament is in the semi-liquid state. The resolution of the printed part produced by common FDM is approximately 0.1 mm.[12] While FDM is widely recognized as a cost-effective 3D printing method, its capability to fabricate small-scale bio-inspired features is relatively limited due to its sub-par resolution in microscale manufacturing.[13] Alternatively, SLM is a powder-based AM technique, which fuses the uniformly spread metallic powder with a high-power laser to produce the metallic structure layer-by-layer.[14] It enables the fabrication of metallic bio-inspired hydrophobic structures with high strength, enhanced impact resistance, and high thermal conductivity.[15] For instance, Mekhiel et al. showcased a 3D printing bio-inspired structure utilizing partially fused stainless steel microparticles to achieve hydrophobicity on a 3D printed metal structure.[16] However, the resolution of SLM products is based on the laser beam spot size, which is typically about 70 to 200 μm.[14] The spatial arrangement of hierarchical features may suffer from some imprecision and inconsistency due to irregular particle size and thermal cycling. Conversely, DLP is a projection-based AM technique utilizing liquid photosensitive resin, which is selectively cured by controlled ultraviolet (UV) light exposure, to print a 3D structure in a layer-by-layer formation. It is capable of producing polymer-based bio-inspired structures with a resolution ranging from 15 μm to 100 μm.[17] Davoudinejad et al. fabricated gecko-inspired adhesive surfaces, featuring two- or three-leveled hierarchical micro-pillars, via UV polymerization, demonstrating high contact angle of water.[18] However, the printed feature using DLP tends to be significantly larger than the natural counterparts, and achieving complex geometries can be challenging.

Hence, the pursuit of a reliable method to accurately fabricate 3D microstructures has become imperative. Two-photon polymerization (TPP) emerges as a promising sub-microscale AM technique, where a small spatial region within the liquid photosensitive resin is polymerized when two photons are simultaneously absorbed by activating lasers.[19] The polymerization process initiates when the absorbed energy of the photosensitive resin surpasses a specific threshold. The photosensitive material around the center of the laser's focal point is solidified to form an ellipsoidal particle, namely a voxel, because of the crosslinking of the polymer chains.[20] The diameter of voxel gradually diminishes vertically, forming a parabolic shape due to the non-linear reduction in energy intensity away from the focal point, eventually dropping below the polymerization energy threshold. As a result, the printed structures consist of periodically arranged voxels based on the laser scanning path according to the programmed digital file. Additionally, the voxel size depends on factors such as type of objective lens, as well as the optimal combination of laser scanning speed and power. Both horizontally and vertically, multiple neighboring voxels overlap with optimal hatching and slicing distances to form a stable structure. The superior resolution of TPP enables the fabrication of numerous bio-inspired structures. For instance, lotus-inspired topography and Salvinia-inspired structures, featuring arrays of papillae and exhibiting hydrophobicity, have been manufactured.[6, 21] Moreover, springtail-skin-inspired designs have demonstrated liquid repellency in dry adhesive structures by adding the double re-entrant feature to the T-shaped fibrillar.[4, 22]

However, the aforementioned bio-inspired hydrophobic surfaces possess limited functionality due to their isotropic design. Although the fabricated hierarchical structure may exhibit properties like self-cleaning and anti-icing, directional controllability is lacking. By modifying the microstructures to incorporate an anisotropic design, programmable surface hydrophobic properties can be introduced. The different directions of liquid movement can be granted by imitating the anisotropic texture of biological surfaces. For example, the movement of the droplets can be directed by allowing the droplets to move towards the far edge of the butterfly wing effortlessly. As the wing is tilted upward and downward, the area of the scales in contact with the droplet increases and decreases accordingly due to the compliant scales rearrangement, which results in anisotropic wettability.[1] Additionally, the droplet sits above the hierarchical surface structures to prevent water accumulation on the body. They can smoothly move along the roll-off direction and collect contaminants, reducing excess weight and enhancing self-cleaning ability. The roll-off direction of the butterfly wing's scale horizontally orientates from the scale root to the tip. Each scale typically measures approximately 180 μm in length, 70 μm in width, and 3 μm in thickness.[8] Smaller features known as lamella-stacking ridges can be found on top of each scale. These lamella-stacking ridges play an integral role in influencing the hydrophobicity of the wing surface, and their dimensions are about 0.7 μm in width, 2 μm in height, and 0.22 μm in stacking spacing.[23]

In this work, inspired by the anisotropic scale design of the Morpho aega butterfly wing, artificial surfaces for directional surface wetting are fabricated via the TPP process. The interplay among TPP printing quality, architecture design, and anisotropic hydrophobic performance are investigated. Particularly, the printing process is optimized to improve the geometrical accuracy of simplified lamella-stacking ridges and the spatial arrangement of artificial wing scales. Furthermore, the hydrophobicity of the printed structures is investigated through the analysis of the contact angle of water. Moreover, anisotropic adhesion is quantified by measuring the minimum required air pressure to move a water droplet under various tilting conditions ranging from 0° to 90° and in two distinct directions, namely roll-off and roll-against directions. Surprisingly, the results reveal a reverse behavior of the artificial surfaces in contrast to their natural counterparts, possibly caused by the significant difference in equilibrium wettability between the Parylene coating and the natural butterfly wing scale surfaces. It is anticipated that the findings will facilitate the design of advanced fluid-controllable interfaces applicable in future sub-microscale fluidic devices, directional coatings, and advanced engineered synthetic scaled surfaces.

EXPERIMENTAL SECTION

2.1. Sample Preparation and Fabrication. To prepare for the TPP process, an indium tin oxide (ITO)-coated square glass substrate (25 mm×25 mm×0.7 mm) is thoroughly cleaned sequentially in deionized (DI) water bath, 99.5% acetone bath, and 99.9% isopropyl alcohol (IPA) bath in a sonicator for 3, 3, 8 minutes, respectively. Next, the surface of the cleaned ITO glass is activated using an oxygen plasma treatment with the Plasma Etch PE-50HF system (Plasma Etch, Caron City, USA) for 40 seconds. Then, a drop of IP-S photoresist (Nanoscribe, Eggenstein-Leopoldshafen, Germany) is deposited at the center of the ITO glass, which is secured onto the substrate holder using polyimide tape. The substrate holder is inserted into the TPP printer with the cleaned 25x objective lens installed. The 25x objective lens is positioned in contact with the photoresist to initiate the polymerization of the liquid photosensitive resin using a laser beam. The fabricated microstructures are then taken out from the printer and developed in propylene glycol methyl ether acetate (PGMEA) (Merck KGaA, Darmstadt, Germany) for 20 minutes to dissolve any uncured excess photosensitive resin. Subsequently, the structures are bathed in IPA for 5 minutes to clean off any remaining PGMEA residue.

2.2. Hydrophobic Parylene Coating. Based on previously reported work, microwave-assisted chemical vapor deposition (CVD) is utilized to apply a Parylene-N hydrophobic coating onto the artificial butterfly scale structures and a cleaned silicon wafer.[24] The thickness of resulting coating is approximately 55 nm as measured from the silicon wafer**.**

2.3. Scanning Electron Microscopy. The quality of the printed microstructures is inspected utilizing an FEI Quanta 650 scanning electron microscopy (SEM). To enhance imaging quality, a thin layer of gold is uniformly coated onto the samples using a 108 Manual sputter coater (Ted Pella, Redding, USA). The SEM imaging is performed in high vacuum mode, at an acceleration voltage of 10 kV to minimize the influence of atmospheric interference.

2.4. Equilibrium Contact Angle Measurement. The equilibrium contact angle measurements are carried out using a digital microscope (AF4915ZTL, Dino-Lite) with a maximum magnification of 140x. All measurements are conducted under controlled environmental conditions. For the static contact angle measurement, a 0.5 μL DI water droplet is transferred by a micropipette and dispensed onto the microstructures within the designated 5×5 mm^2 printed area. The contact angles are measured using ImageJ software at a view perpendicular to the artificial scales' roll-off direction.

2.5. Roll-off and Roll-against Pressures Measurement. A rotational stage is securely mounted vertically on a flat wall surface, and a custom-made substrate holder is attached to the rotational stage. Then, the substrate containing the printed microstructures is placed horizontally on the holder, and the roll-off direction of microstructures is perpendicular to the rotation axis of the stage. Following that, a pneumatic nozzle, connecting to Ultimus II dispenser (Nordson EFD, USA), is positioned perpendicularly to the edge of the printed surface with 35 mm distance, and a 0.5 µL DI water droplet is deposited on the edge close to the pneumatic nozzle. With this setup, a stable airflow is generated via the pneumatic nozzle, and the minimum required pressure to initialize droplet motion is measured. When the airflow direction is along the roll-off direction, the roll-off pressure (ROP) is determined when the DI water droplet shifts along the airflow direction. Likewise, roll-against pressure (RAP) is measured in the reverse roll-off direction. The experiment setup can be found in supporting information (Figure S1).

RESULT AND DISCUSSION

The scales on the natural wings of the Morpho aega butterfly are arranged in a radial outward orientation from the body, overlapping in a manner similar to that of roof shingles, as shown in Figure 1a-c. The average length and width of the butterfly wing's scale are approximately 180 µm and 72 µm, respectively, which aligns with values presented in another research.[8] Inspired by the scale of butterfly wing, the curved microstructure featuring ridges is designed based on the dimensions of the natural wing scale (Figure S2, Supporting Information). Arc length similar to the scale of Morpho aega butterfly wing is achieved by setting the length to 150 µm and root tilted angle to 120 °. Considering all the above dimensions, the overall height of the fabricated structure is about 98 µm. The width of the curved scale is set to 72 µm to ensure even distribution of the ridge structure into grating pitches (γ) of 4 μm, 8 μm, and 12 μm. The lamella-stacking ridge nanostructure is simplified to a single ridge with 5 μm height. The thickness of the artificial scales is set to 10 μm to avoid degradation in structure due to overhanging. The base with 12 μm thickness supports the artificial scale structures to avoid detachment from the built plate. A gap with half the grating pitch is added between each scale structure perpendicular to the direction of the scale. The base width is equivalent to the sum of the scale width and the gap. An array group of artificial scales is designed with varying base lengths (L) of 70 μm, 80 μm, and 90 μm. A total of nine designs with varying grating pitches γ and base length L are fabricated and further studied.

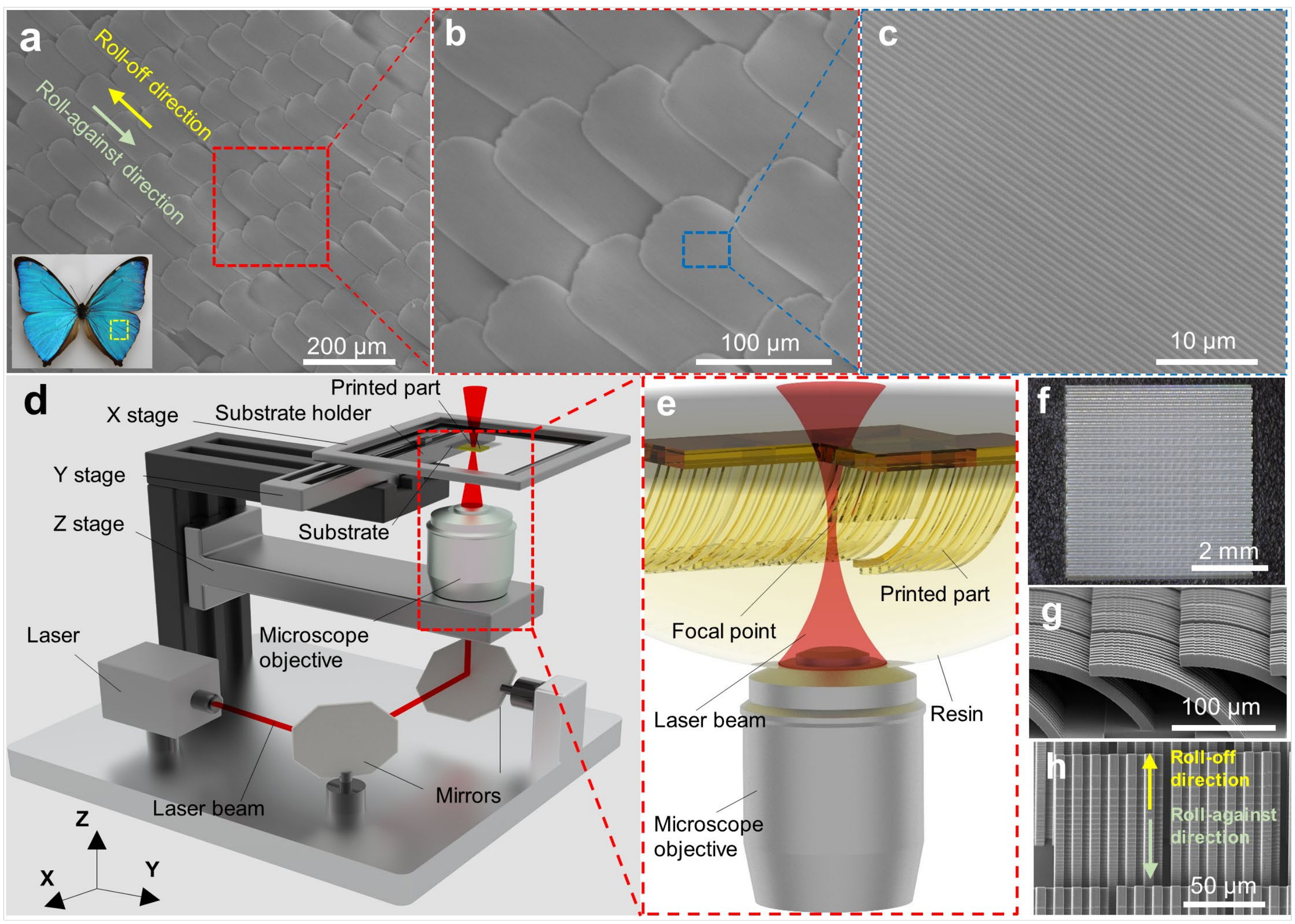

Figure 1. (a)-(c) SEM image of the natural butterfly wing. (d) Schematic diagram of the TPP 3D printer. The microscope objective moves along the z-axis, and the substrate can move in the xy-plane. Two mirrors control the laser beam scanning path in the xy-plane. (e) Schematic diagram of the

artificial butterfly scale microstructures printing process. The microscope objective is immersed in photosensitive resin, and the liquid resin at the focal point of the laser beam is polymerized. (f) Patterned artificial butterfly scales on ITO-coated glass substrate. (g)-(h) SEM images of the top and side views of the printed microstructures.

As shown in Figure 1d, for the specific TPP printer used in imitating the scale of butterfly wing, the Nanoscribe Photonic Professional GT2 system (Nanoscribe, Eggenstein-Leopoldshafen, Germany) employs an objective lens to fabricate microstructures. In the process, laser pulses are generated by a near-infrared laser beam in a TPP printer and used to excite the photoinitiator molecules in the photosensitive material.[25] To ensure structural stability, the smallest feature in the design, which is the ridge structure with 2 μm width, requires at least three neighboring voxels to support the weight of a water droplet. Therefore, the 25x objective lens, capable of fabricating microstructures with a voxel size of 600 nm in diameter and 3.6 μm in height, is necessary and more suitable for efficient printing of the designed artificial scale surfaces.

The computer-aided design (CAD) model of the artificial scale surface is processed by the 3D slicer DeScribe software with the default settings for the 25x objective lens using 1 μm slicing distance and 0.5 μm hatching distance. Then, the artificial butterfly scale is printed in a bottom-up matter, starting from the scale root to the scale tip (Figure 1e). During the process, voxel fusion occurs parallel to the roll-off direction to prevent the formation of floating polymerized particles when dealing with overhanging features. To establish a robust bond between the printed structures and the substrate, the number of base layers is set to 6 with 80% laser power. As a result, the anisotropic scale surface, inspired by the scales of Morpho aega butterfly wing, with 5×5 mm^2 is successfully fabricated on an ITO glass (Figure 1f). The artificial scales are neatly arranged with specific offset and spacing with the same orientation as designed (Figure 1g,h).

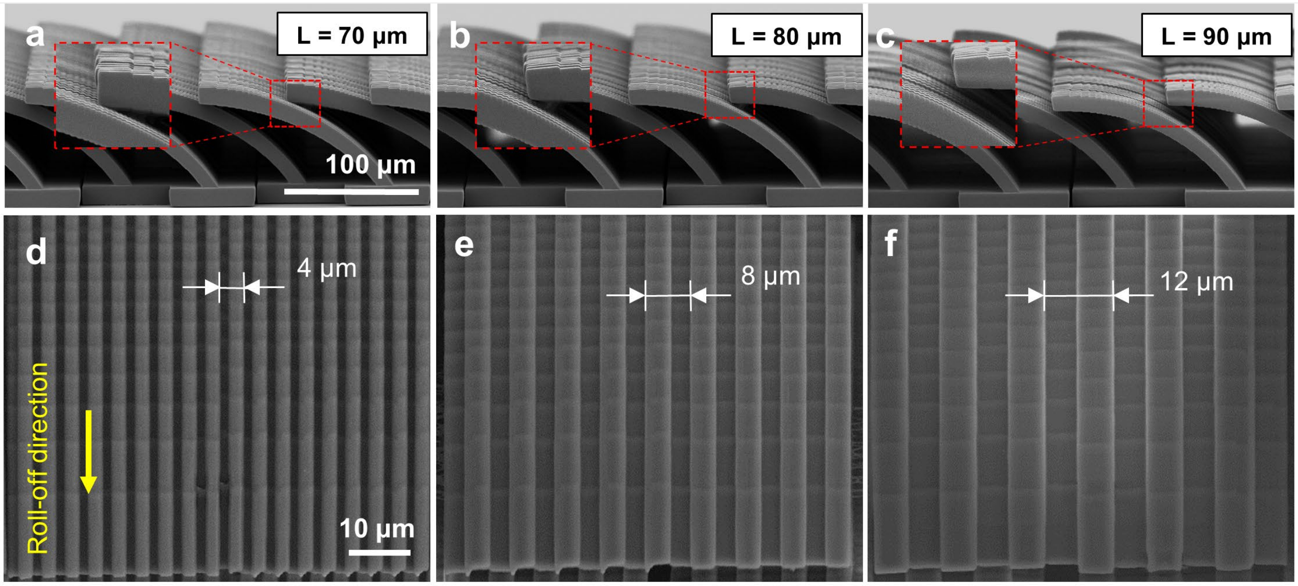

Figure 2. SEM of TPP printed artificial scales. (a)-(c) Side views of the designs with $\gamma = 6$ µm, and L= 70 µm, 80 µm, and 90 µm. (d)-(f) Top view of the tip of the artificial scales with $\gamma = 4$ µm, 8 µm, and 12 µm.

Figure 2a-c shows the side views of the TPP fabricated microstructures inspired by the scale of butterfly wing. It can be observed that, when the base length is set to 70 µm, the tip of the printed scales is in contact with the neighboring scales in the roll-off direction. The vertical gaps between two adjacent scales for the 80 µm and 90 µm base length sets are about 5 µm and 10 µm, respectively. As shown in Figure 2d-f, additive layers can be observed easily on the top of the scales. Smoother curvature can be printed by reducing the slicing distance, but the required fabrication time increases drastically. The printed ridge structures on the artificial scales match the designed grating pitches 4 µm, 8 µm, and 12 µm. For all designs, the difference between the width of the peaks and valleys is measured to be 2 µm.

An optimized printing strategy is crucial due to the effect of microstructures' quality on hydrophobic performance.[8] The quality of the printed artificial scales can be improved by modifying the objective movement and laser scanning paths. Specifically, the objective lens moves along or against the roll-off direction to fabricate once a row of scales is fabricated (Figure 3a). When the objective is positioned at the desired location, the laser is activated and polymerizes the photoresist with a programmed scanning path (Figure 3b). During the printing process, voxel fusion occurs along the roll-off direction to prevent the formation of floating polymerized particles when dealing with overhanging features.

As demonstrated in Figure 3c-e, two different laser scanning paths are tested, namely back-and-forth and one-way paths. The resulting morphologies of the printed scales are shown separately in Figure 3c,e. In Figure 3c, two fused voxels are observed at the end of the hatching lines because the photopolymer resin is exposed to the laser for a longer duration when reversing the scanning direction to print the next hatching line. On the contrary, the quality of the microstructures is improved by setting the laser scanning path to one-way, and the protuberant features are precluded, as shown in Figure 3e. However, compared with the back-and-forth laser scanning path, alternating laser scanning with a one-way path significantly increases the fabrication time due to the discontinuous printing path.

Additionally, the objective lens moving path is a factor affecting the quality of the fabricated microstructures. As shown in Figure 3f-g, the laser penetrates the completed structure if the objective lens moves along the roll-off direction when fabricating a new row of artificial scales. The printed structure underneath the adjacent fabricated scale mismatches the design due to the refraction of the laser and shifted focal point. The differences between the printed microstructures and the designs, such as detachment from ITO glass substrate, misalignment between the base structures, and discontinuous curved surface of the artificial scale, can be precluded by moving the objective lens along the roll-against path when printing the next row of artificial scales as shown in Figure 3h.

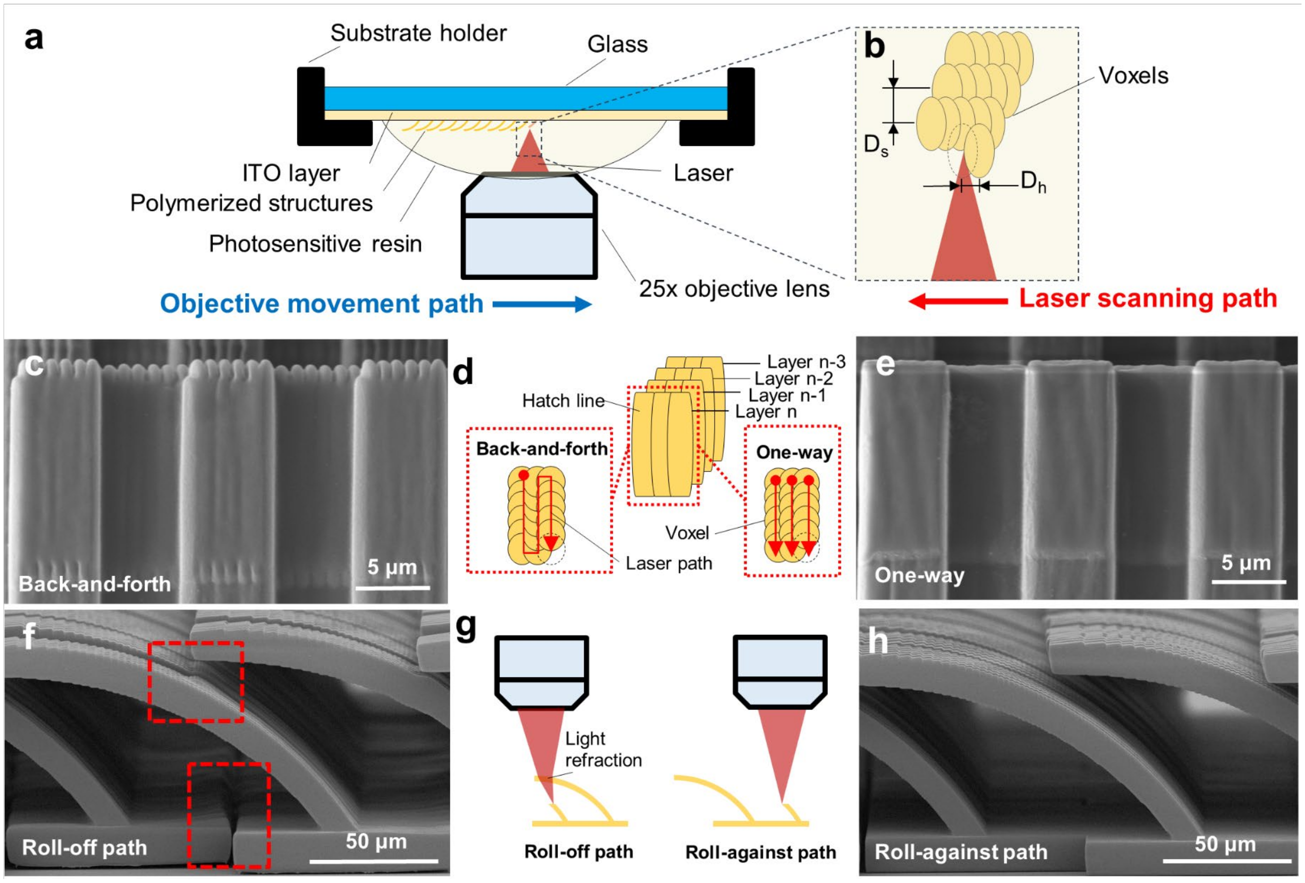

Figure 3. (a) Artificial scales are fabricated on an ITO-coated glass with a 25x objective lens moving along the roll-against direction. (b) Voxels polymerization at the laser focal point and the laser scan along the roll-off direction. (c)-(e) Schematic of a typical hatch line fabrication via voxel fusing with back-and-forth and one-way laser scanning paths, and SEM of the artificial scales tip with $\gamma = 12$ µm printed via the corresponding scanning paths. (f)-(h) Schematic of the objective moving path and the corresponding laser focal point while fabricating adjacent microstructures, and SEM of the side of the artificial scales with $\gamma = 12$ µm printed via roll-off and roll-against objective moving paths.

To demonstrate water droplets can roll off from the surface, the printed microstructures need to have hydrophobicity, which can be determined based on the contact angle of water. The equilibrium contact angles of water droplets on all the surfaces with different dimensions of artificial scales are measured as previously described. The surfaces investigated include an ITO-coated glass, Parylene-N-coated glass, as well as non-coated and Parylene-N coated microstructures. As depicted in Figure 4a,b, the contact angles of the ITO-coated glass and the Parylene-N coated glass are about 39° and 92°, respectively. As illustrated in Figure 4c, while the IP-S photoresist microstructures elevate the contact angle, nearing the effect seen with the Parylene-N coated glass, they fail to realize optimal hydrophobicity. The liquid penetrates the gaps of the artificial scales, which agrees with the mechanism for surface wetting on the hierarchical structure in Wenzel states.[26]

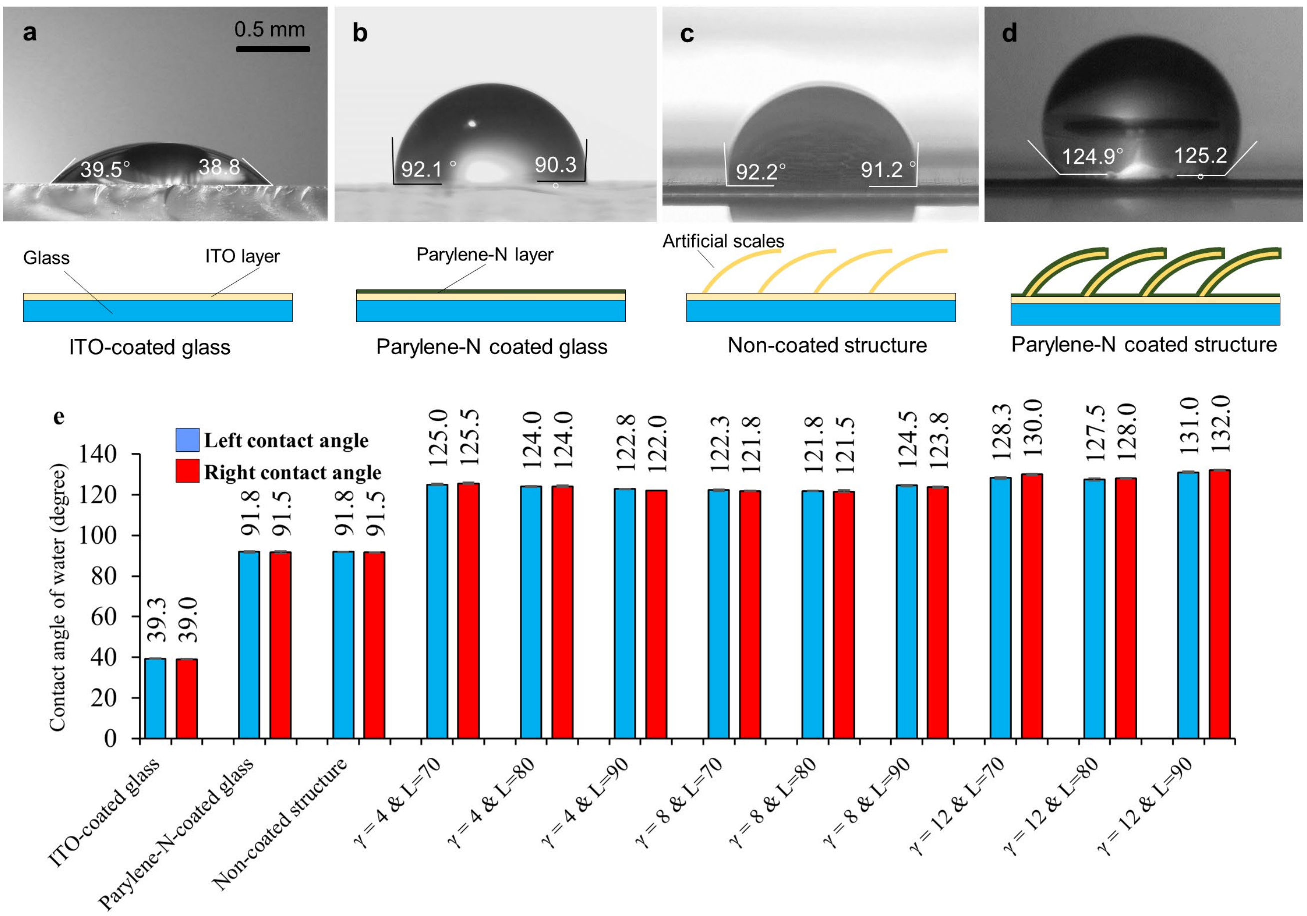

Figure 4. Water contact angle measurement. (a)-(b) the contact angle of water of ITO-coated and Parylene-N coated glass (c)-(d) The contact angle of water of non-coated and Parylene-N coated microstructure design with $\gamma = 4$ µm and $L = 70$ µm design. (e) Left and right average contact angles of ITO-coated glass, Parylene-N coated glass, non-coated artificial scale microstructures, and the coated microstructures with different design parameters.

Consequently, an additional slender Parylene-N layer is incorporated to boost the hydrophobic attributes. Figure 4d shows the addition of a 55 nm thick Parylene-N coating drastically increased the water greater than 120° for the printed artificial scales. The water droplet is supported by the air that is trapped in the gap, which matches the mechanism for surface wetting on the hierarchical structure in Cassie-Baxter state.[26] As Figure 4e shows, the microstructure surfaces with 4 μm and 8 μm grating pitches had similar contact angles ranging from 121.5° to 125.5°. The 12 μm grating pitch design had the highest level of hydrophobicity with contact angles ranging from 127.5° to 132.0°. A complete measurement of contact angle of water of Parylene-N coated microstructure designs can be found in supporting information (Figure S3 and Table S1)

To test the anisotropic properties of the fabricated surfaces, air pressure is applied to the water droplet to observe the effect of the microstructures on liquid movement in different directions. More specifically, the anisotropic behavior of the microstructures is characterized by analyzing droplet's mobility under various tilting conditions at 0°, 30°, 60°, and 90°. The anisotropic liquid transportability is determined through the minimum required air pressure to initiate water droplet movement in roll-off and roll-against directions, namely ROP and RAP.

As shown in Figure 5a, the pressure required to move droplets in roll-against direction is significantly less than the roll-off direction, which is opposite to the natural butterfly wing scale. It should be noted that previous research demonstrated that the water droplet on the artificial wing scale could naturally move along the roll-off direction when the equilibrium contact angle was larger than 150°.[8] Unexpectedly, in this study, the water droplet is pinned on the surface without the assistance of airflow, regardless of the variation in grating pitch and base length. Potential cause of this effect can be lack of high enough hydrophobicity of the surfaces to let the water droplet naturally roll down.

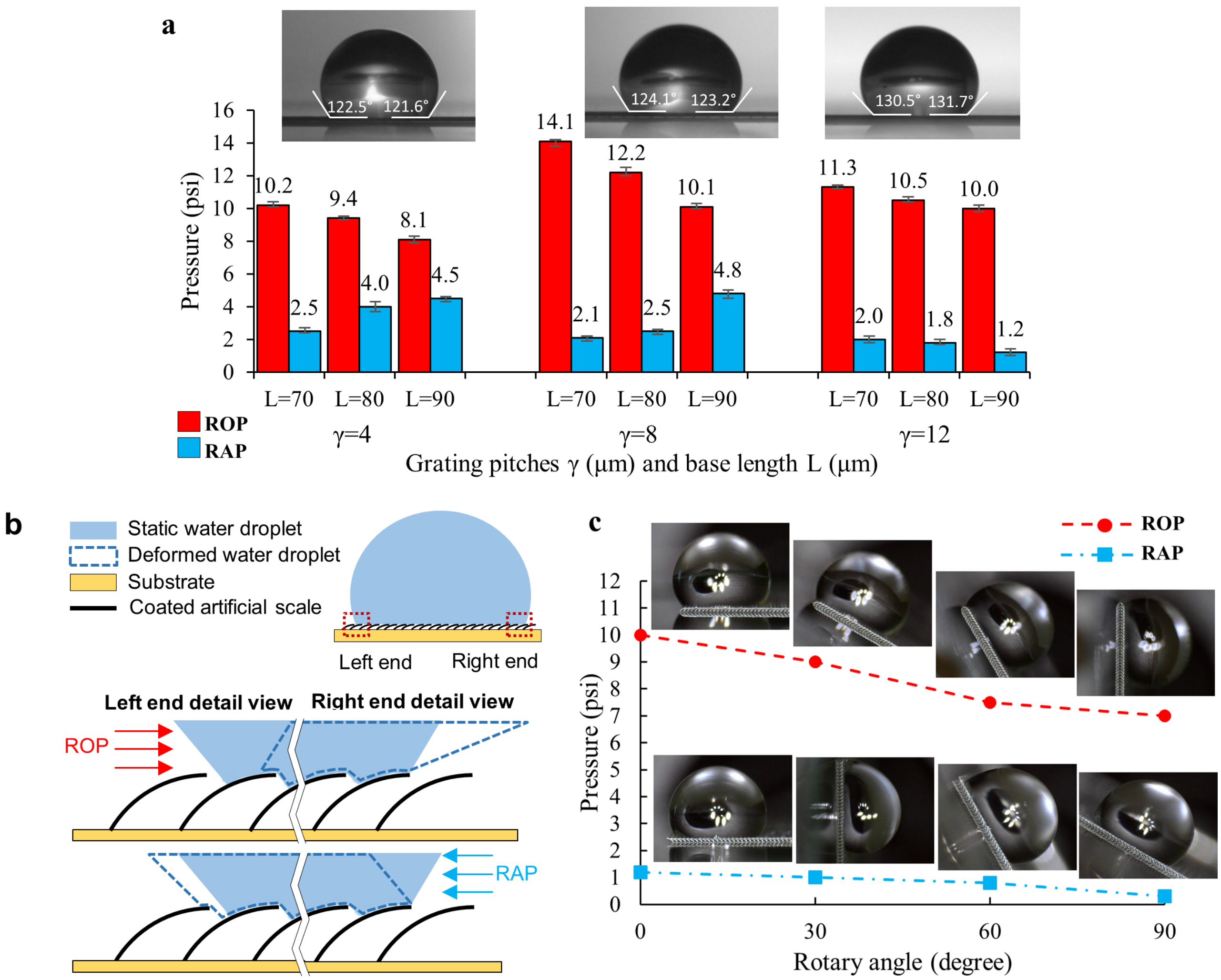

Figure 5. ROP and RAP measurements at various degrees and schematic of water droplet movement under air pressure. (a) ROP and RAP for different γ and L at 0° of rotation. (b) Schematic of liquid transportation on artificial scale surface with applied air pressure. A water droplet sits on the microstructures and presents hydrophobicity in a steady state. Detail views of the droplet's deformation under ROP and RAP at the left and right ends. (c) Average ROP and RAP for γ = 12 μm and L = 90 μm at 0°, 30°, 60°, and 90° of rotation.

Figure 5b shows a schematic of a droplet demonstrating Cassie-Baxter state surface wetting. RAP is used to push the droplet to slide towards the scales' decline direction and make the droplet in contact with the nearby microstructures. In contrast, ROP is applied to support the droplet to move towards the scales' incline direction and cause the droplet to fall and sit onto the adjacent artificial scales, which requires more energy to exceed the hydrostatic equilibrant at the tip as well as overcome the potential energy of the droplet. As the base length increased from 70 μm to 80 μm, and lastly to 90 μm, the contact angle of water had minor changes within 1° difference, but the ROP decreased significantly. The decrease in ROP is possibly due to reducing the number of artificial scales in contact with the droplet, resulting in lower resistance in movement. Specifically, for the 4 μm and 8 μm grating pitch design, RAP is increased as the base length increases. This is possibly caused by the increasing gaps between the artificial scales trapping the droplet. On the contrary, for the 12 μm grating pitches design, RAP is decreased with a decrease in the base length. The higher contact angle of water presented in the 12 μm grating pitch design perhaps lowers the required energy for the droplet to slide toward the roll-off direction and jump onto the adjacent scales. In addition, ROP and RAP are decreased as the rotary angle of the stage increased because the increased gravitational potential energy along the roll-off direction reduced the need for pressure for water droplet shift to the adjacent artificial scales, as shown in Figure 5c. Both ROP and RAP are measured for the surfaces with different printed microstructures at 0°, 30°, 60°, and 90°, a complete measurement can be found in supporting information (Table S2).

To explore the possibility of the proposed bio-inspired microstructures for innovative water-related energy harvesting and droplet manipulating devices,[27, 28] as a test case, a functional hydrophobic surface with multiple anisotropic liquid transportation directions is designed. The surface is divided into three regions with different roll-against directions (Figure 6a). The roll-against directions of Regions I, II, and III are oriented differently, and their geometrical designs (base length L and grating pitches γ) are based on the measurement of ROP and RAP. It should be noticed that all the designs have the same base length, L = 70 μm. Specifically, Region I consists of the design with the highest ROP (γ = 8 μm), providing strong resistance to water droplet motion and limiting the droplet rolling across the boundary when airflow is applied from the front and air pressure is lower than 14.1 psi.

Regions II and III consist of the design with the lowest RAP (γ = 12 μm) with the same base length, avoiding undesired gaps between the three regions. This design also enables droplets to roll from the back to the front of Region II and right to left of Region III when air pressure is higher than 2 psi. According to the aforementioned designs (γ = 8 μm and γ = 12 μm), a 1×1 cm^2 surface is fabricated via TPP (Figure 6b,c).

To further demonstrate the anisotropic hydrophobicity behaviors, the water droplets, on top of the horizontally placed fabricated artificial surface, are tested under airflow generated by two pneumatic nozzles. Specifically, two nozzles are separately positioned 35 mm away from the front and right edges of the fabricated surface. They are connected to an air dispenser which is set to provide a consistent 5 psi air pressure, pointing to the roll-against direction of Region II and III (Figure 6d). In addition, to push all the water droplets distributed along the front edge of the printed surface, the front nozzle moves perpendicular to roll-against direction of Region II and remains the 35mm distance for the fabricated surface.

In this study, to investigate the behavior of anisotropic transportability of the proposed design, six droplets are initially deposited on left and right segments ("3+3") in Region II (Figure 6e). Under the external airflow, we noticed that the deposited water droplets are moved and accumulated together as the width of Region II decreases (Figure 6f). Subsequently, the majority portion of the accumulated droplet moves within Region II along its roll-against direction. The remaining portion of the water droplets pinned by the microstructures in Region I is dragged by the water surface tension and moves along the boundary of Region II. Afterward, the motion of the accumulated droplet is pinned on Region III due to the designed roll-against direction (Figure 6g). Finally, the pinned water droplets are moved by the stationary airflow generated by the side nozzle and removed from the fabricated surface (Figure 6h).

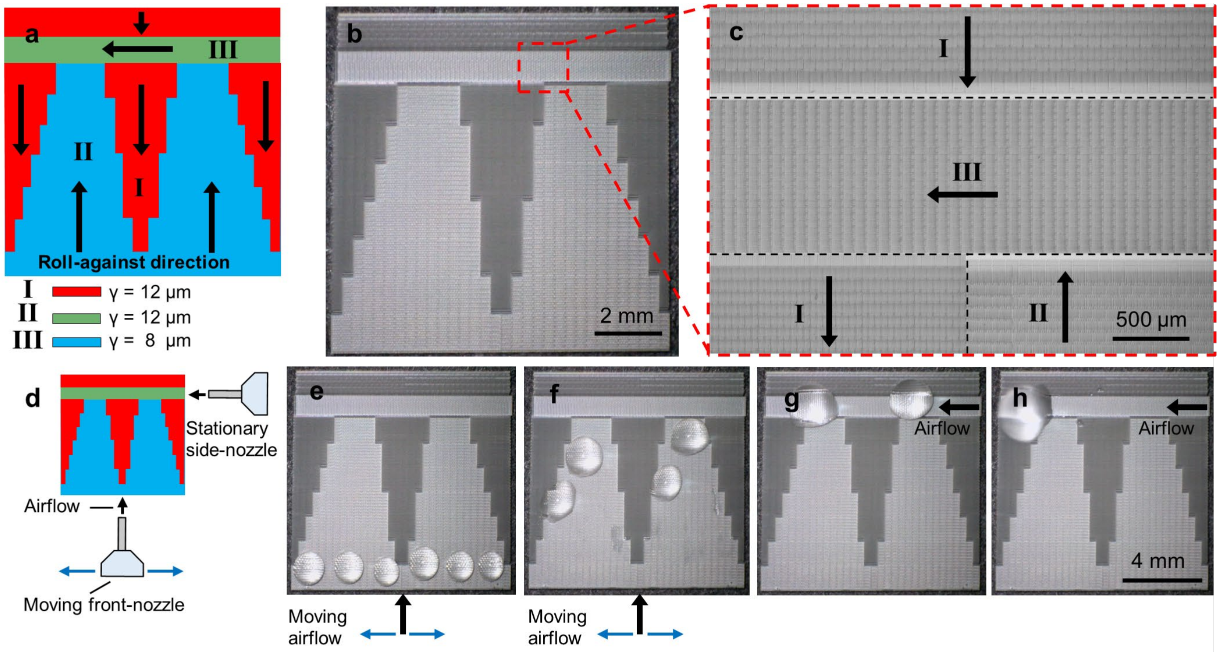

Figure 6. Demonstration of a functional hydrophobic surface for liquid transportation. (a) A printed microstructure surface consisting of two designs of artificial scale in three orientations. The design with γ = 12 µm and L = 70 µm are arranged in Regions II and III, and the design with γ = 8 µm and L = 70 µm are patterned in the red regions. (b) Six drops of DI water are deposited on the printed microstructures. (c)-(d) Droplets are moved and merged as the airflow is applied along the roll-against direction of Region II, and Region I stops the droplets. (e) The droplets are moved and merged as the airflow is applied along the roll-against direction of Region III.

According to the observation, the synthetic bio-inspired hydrophobic surface demonstrates the capability of transporting water droplets along the roll-against direction by pinning droplets in undesired regions until supplied airflow aligns with favorable regions. In addition, the "1+1" and "2+2" droplet patterns are also tested under the same conditions, and the results are included in supporting information (Figure S4-S5). From these findings, effective controllable fluid transportation can be achieved by fabricating engineered hydrophobic surfaces, using multiple designs based on Morph aega butterfly scale via TPP. Such engineered structures coupled with advanced AM can facilitate the implementation of applications, such as energy harvesting and droplet manipulating devices.

CONCLUSIONS

In this article, inspired by scales of butterfly wings, various 3D hydrophobic microstructure surfaces are fabricated on ITO-coated glass slides using the TPP technique. The quality of the artificial butterfly scale is improved by implementing a one-way laser scanning strategy and making adjustments to the objective lens movement in alignment with the roll-against direction during printing. The fabricated microstructures enhance the hydrophobicity of the surfaces and significantly increase the contact angle of water when coated with a thin layer of Parylene-N. The hydrophobicity is further improved by increasing the grating pitch length of the ridge structure on the artificial scales. With the hydrophobic coating, anisotropic drop adhesion is presented on the engineered 3D structured surface, which showcases less favor to move along the roll-off direction than along the roll-against direction, opposite to the natural counterparts. In terms of the geometrical parameters, the increase in base length of the printed scales improves the movability of the droplet. Still, it encounters more difficulty in moving along the roll-against direction due to reduced hydrophobicity. The presented TPP printed scale surfaces with directional adhesion hold potential for various applications, such as tunable fluid transport surfaces, self-cleaning exteriors, and micro-channel filling. Future work may include modeling the droplet movement on the artificial scale to determine the optimal dimensions for reducing resistance in the roll-against direction.

■ ASSOCIATED CONTENT

Supporting Information

Experimental setup for roll-off and roll-against pressures measurement; CAD models of butterfly-inspired artificial scales; Contact angle of water on Parylene-N coated microstructure designs; The

“1+1” and “2+2” droplet patterns tested on functional hydrophobic surface; Contact angles of water measurements; Measurement of ROP and RAP of Parylene-N coated microstructures.

■ AUTHOR INFORMATION

Corresponding Authors:

*__Meng Cheng__ - Key Laboratory of Metallurgical Equipment and Control Technology, Ministry of Education, Wuhan University of Science and Technology, Wuhan, Hubei 430081, China

*__Daewon Kim__ - Department of Aerospace Engineering, Embry-Riddle Aeronautical University, Daytona Beach, FL 32114, United States; Email: daewon.kim@erau.edu

*__Yizhou Jiang__ - Department of Aerospace Engineering, Embry-Riddle Aeronautical University, Daytona Beach, FL 32114, United States; Email: yizhou.jiang@erau.edu

Authors

∇**Zefu Ren** - Department of Aerospace Engineering, Embry-Riddle Aeronautical University, Daytona Beach, FL 32114, United States

∇**Zhuoyuan Yang** - Department of Aerospace Engineering, Embry-Riddle Aeronautical University, Daytona Beach, FL 32114, United States

Rishikesh Srinivasaraghavan Govindarajan - Department of Aerospace Engineering, Embry-Riddle Aeronautical University, Daytona Beach, FL 32114, United States

Foram Madiyar - Department of Physical Science, Embry-Riddle Aeronautical University, Daytona Beach, FL 32114, United States

Author Contributions

∇These authors contributed equally to this work. The manuscript was written through contributions from all authors. All authors have approved the final version of the manuscript.

Notes

The authors declare that the research was conducted in the absence of any commercial or financial relationships that could be construed as a potential conflict of interest.

■ ACKNOWLEDGMENTS

This material is based upon work supported partially by the National Science Foundation under Grants No. 2018853 and 2050887, and Natural and Science Foundation of China under Grant No. 52201272. The opinions, findings, and conclusions, or recommendations expressed are those of the authors and do not necessarily reflect the views of the National Science Foundation and Natural and Science Foundation of China.

■ REFERENCES

(1) Zheng, Y.; Gao, X.; Jiang, L. Directional adhesion of superhydrophobic butterfly wings. *Soft Matter* **2007**, *3* (2), 178-182.

(2) Lv, J.; Song, Y.; Jiang, L.; Wang, J. Bio-Inspired Strategies for Anti-Icing. *ACS Nano* **2014**, *8* (4), 3152-3169.

(3) Plamadeala, C.; Gosain, S. R.; Hischen, F.; Buchroithner, B.; Puthukodan, S.; Jacak, J.; Bocchino, A.; Whelan, D.; O'Mahony, C.; Baumgartner, W.; et al. Bio-inspired microneedle design for efficient drug/vaccine coating. *Biomedical Microdevices* **2019**, *22* (1), 8.

(4) Dayan, C. B.; Chun, S.; Krishna-Subbaiah, N.; Drotlef, D.-M.; Akolpoglu, M. B.; Sitti, M. 3D Printing of Elastomeric Bioinspired Complex Adhesive Microstructures. *Advanced Materials* **2021**, *33* (40), 2103826.

(5) Yang, L.; Shen, X.; Yang, Q.; Liu, J.; Wu, W.; Li, D.; Du, J.; Zhang, B.; Fan, S. Fabrication of biomimetic anisotropic super-hydrophobic surface with rice leaf-like structures by femtosecond laser. *Optical Materials* **2021**, *112*, 110740.

(6) Lantada, A. D.; Hengsbach, S.; Bade, K. Lotus-on-chip: computer-aided design and 3D direct laser writing of bioinspired surfaces for controlling the wettability of materials and devices. *Bioinspiration & Biomimetics* **2017**, *12* (6), 066004.

(7) Tellechea-Robles, L. E.; Méndez-Alonzo, R.; Molina-Freaner, F. E.; Maldonado, A. Microstructure and Hydrophobicity of the External Surface of a Sonoran Desert Beetle. *Biomimetics* **2022**, *7* (2), 38.

(8) Zhao, H.; Park, S. J.; Solomon, B. R.; Kim, S.; Soto, D.; Paxson, A. T.; Varanasi, K. K.; Hart, A. J. Synthetic Butterfly Scale Surfaces with Compliance-Tailored Anisotropic Drop Adhesion. *Advanced Materials* **2019**, *31* (14), 1807686.

(9) Yoon, Y.; Kim, D.; Lee, J.-B. Hierarchical micro/nano structures for super-hydrophobic surfaces and super-lyophobic surface against liquid metal. *Micro and Nano Systems Letters* **2014**, *2* (1), 3.

(10) Xu, Y.; Mao, H.; Liu, C.; Du, Z.; Yan, W.; Yang, Z.; Partanen, J.; Chen, Y. Hopping Light Vat Photopolymerization for Multiscale Fabrication. *Small* **2023**, *19* (11), 2205784.

(11) Joyee, E. B.; Pan, Y. Multi-material Additive Manufacturing of Functional Soft Robot. *Procedia Manufacturing* **2019**, *34*, 566-573.

(12) Khan, S.; Joshi, K.; Deshmukh, S. A comprehensive review on effect of printing parameters on mechanical properties of FDM printed parts. *Materials Today: Proceedings* **2022**, *50*, 2119-2127.

(13) Xing, R.; Yang, B.; Huang, R.; Qi, W.; Su, R.; Binks, B. P.; He, Z. Three-Dimensionally Printed Bioinspired Superhydrophobic Packings for Oil-in-Water Emulsion Separation. *Langmuir* **2019**, *35* (39), 12799-12806.

(14) Gu, D.; Shi, X.; Poprawe, R.; Bourell, D. L.; Setchi, R.; Zhu, J. Material-structure-performance integrated laser-metal additive manufacturing. *Science* **2021**, *372* (6545), eabg1487.

(15) Yang, J.; Gu, D.; Lin, K.; Zhang, Y.; Guo, M.; Yuan, L.; Zhang, H.; Zhang, H. Laser Additive Manufacturing of Bio-inspired Metallic Structures. *Chinese Journal of Mechanical Engineering: Additive Manufacturing Frontiers* **2022**, *1* (1), 100013.

(16) Mekhiel, S.; Koshy, P.; Elbestawi, M. A. Additive texturing of metallic surfaces for wetting control. *Additive Manufacturing* **2021**, *37*, 101631.

(17) Li, H.; Dai, J.; Wang, Z.; Zheng, H.; Li, W.; Wang, M.; Cheng, F. Digital light processing (DLP)-based (bio)printing strategies for tissue modeling and regeneration. *Aggregate* **2023**, *4* (2), e270.

(18) Davoudinejad, A.; Ribo, M. M.; Pedersen, D. B.; Islam, A.; Tosello, G. Direct fabrication of bio-inspired gecko-like geometries with vat polymerization additive manufacturing method. *Journal of Micromechanics and Microengineering* **2018**, *28* (8), 085009.

(19) Lin, Y.; Zhou, R.; Xu, J. Superhydrophobic Surfaces Based on Fractal and Hierarchical Microstructures Using Two-Photon Polymerization: Toward Flexible Superhydrophobic Films. *Advanced Materials Interfaces* **2018**, *5* (21), 1801126.

(20) Raimondi, M. T.; Eaton, S. M.; Nava, M. M.; Laganà, M.; Cerullo, G.; Osellame, R. Two-photon laser polymerization: from fundamentals to biomedical application in tissue engineering and regenerative medicine. *Journal of applied biomaterials & functional materials* **2012**, *10* (1), 56-66.

(21) Tricinci, O.; Pignatelli, F.; Mattoli, V. 3D Micropatterned Functional Surface Inspired by Salvinia Molesta via Direct Laser Lithography for Air Retention and Drag Reduction. *Advanced Functional Materials* **2023**, 2206946.

(22) Yamaguchi, M. Microfabrication of re-entrant surface with hydrophobicity/oleophobicity for liquid foods. *Scientific Reports* **2020**, *10* (1), 2250.

(23) Watanabe, K.; Hoshino, T.; Kanda, K.; Haruyama, Y.; Kaito, T.; Matsui, S. Optical measurement and fabrication from a Morpho-butterfly-scale quasistructure by focused ion beam chemical vapor deposition. *Journal of Vacuum Science & Technology B: Microelectronics and Nanometer Structures Processing, Measurement, and Phenomena* **2005**, *23* (2), 570-574.

(24) Lichade, K. M.; Jiang, Y.; Pan, Y. Hierarchical Nano/Micro-Structured Surfaces With High Surface Area/Volume Ratios. *Journal of Manufacturing Science and Engineering* **2021**, *143* (8).

(25) Srinivasaraghavan Govindarajan, R.; Stark, T.; Madiyar, F.; Kim, D. On the performance of PVDF based piezoelectric sensor with microstructures. In SPIE Smart Structures + Nondestructive Evaluation, Paper SS, 2023.

(26) Hejazi, V.; Moghadam, A. D.; Rohatgi, P.; Nosonovsky, M. Beyond Wenzel and Cassie–Baxter: Second-Order Effects on the Wetting of Rough Surfaces. *Langmuir* **2014**, *30* (31), 9423-9429.

(27) Lin, Z.-H.; Cheng, G.; Lee, S.; Pradel, K. C.; Wang, Z. L. Harvesting Water Drop Energy by a Sequential Contact-Electrification and Electrostatic-Induction Process. *Advanced Materials* **2014**, *26* (27), 4690-4696.

(28) Tang, X.; Zhu, P.; Tian, Y.; Zhou, X.; Kong, T.; Wang, L. Mechano-regulated surface for manipulating liquid droplets. *Nature Communications* **2017**, *8* (1), 14831.